

Ventilatory capacity in CLAD is driven by dysfunctional airway structure



Pieterjan Kerckhof,^a Gene P. L. Ambrocio,^{a,b} Hanne Beeckmans,^a Janne Kaes,^a Vincent Geudens,^a Saskia Bos,^c Lynn Willems,^a Astrid Vermaut,^a Marie Vermant,^a Tinne Goos,^a Charlotte De Fays,^{a,d} Lucia Aversa,^a Yousry Mohamady,^a Arno Vanstapel,^{a,e} Michaela Orlitová,^f Jan Van Slambrouck,^a Xin Jin,^a Vimi Varghese,^{a,g} Iván Josipovic,^h Matthieu N. Boone,^h Lieven J. Dupont,ⁱ Birgit Weynand,^e Adriana Dubbeldam,^j Dirk E. Van Raemdonck,^k Laurens J. Ceulemans,^k Ghislaine Gayan-Ramirez,^a Laurens J. De Sadeleer,^{a,l} John E. McDonough,^m Bart M. Vanaudenaerde,^{a,n} and Robin Vos^{i,*}



^aLaboratory of Respiratory Diseases and Thoracic Surgery (BREATHE), Department of CHROMETA, KU Leuven, Leuven, Belgium

^bDivision of Pulmonary Medicine, Department of Internal Medicine, University of the Philippines – Philippine General Hospital, Manila, The Philippines

^cNewcastle University, Translational and Clinical Research Institute, Newcastle upon Tyne, United Kingdom

^dPole of Pneumology, ENT, and Dermatology, Institute of Experimental and Clinical Research, Université Catholique de Louvain, Brussels, Belgium

^eDepartment of Pathology, University Hospitals Leuven, Leuven, Belgium

^fDepartment of Cardiovascular Sciences, KU Leuven, Leuven, Belgium

^gDepartment of Heart and Lung Transplant, Yashoda Hospitals, Hyderabad, India

^hDepartment of Physics and Astronomy, UGCT, Radiation Physics, Ghent University, Ghent, Belgium

ⁱDepartment of Respiratory Diseases, University Hospitals Leuven, Leuven, Belgium

^jDepartment of Radiology, University Hospitals Leuven, Leuven, Belgium

^kDepartment of Thoracic Surgery, University Hospitals Leuven, Leuven, Belgium

^lCell Circuits in Systems Medicine of Lung Disease (Schiller Lab), Institute of Lung Health and Immunity (LHI) / Comprehensive Pneumology Centre (CPC), German Centre for Lung Research, Helmholtz Zentrum München, München, Germany

^mDepartment of Medicine, McMaster University, Firestone Institute of Respiratory Health, Hamilton, Canada

Summary

Background Chronic lung allograft dysfunction (CLAD) encompasses three main phenotypes: bronchiolitis obliterans syndrome (BOS), restrictive allograft syndrome (RAS) and a Mixed phenotype combining both pathologies. How the airway structure in its entirety is affected in these phenotypes is still poorly understood.

Methods A detailed analysis of airway morphometry was applied to gain insights on the effects of airway remodelling on the distribution of alveolar ventilation in end-stage CLAD. *Ex vivo* whole lung μ CT and tissue-core μ CT scanning of six control, six BOS, three RAS and three Mixed explant lung grafts (9 male, 9 female, 2014–2021, Leuven, Belgium) were used for digital airway reconstruction and calculation of airway dimensions in relation to luminal obstructions.

Findings BOS and Mixed explants demonstrated airway obstructions of proximal bronchioles (starting at generation five), while RAS explants particularly had airway obstructions in the most distal bronchioles (generation >12). In BOS and Mixed explants 76% and 84% of bronchioles were obstructed, respectively, while this was 22% in RAS. Bronchiolar obstructions were mainly caused by lymphocytic inflammation of the airway wall or fibrotic remodelling, i.e. constrictive bronchiolitis. Proximal bronchiolectasis and imbalance in distal lung ventilation were present in all CLAD phenotypes and explain poor lung function and deterioration of specific lung function parameters.

Interpretation Alterations in the structure of conducting bronchioles revealed CLAD to affect alveolar ventilatory distribution in a regional fashion. The significance of various obstructions, particularly those associated with mucus, is highlighted.

eBioMedicine

2024;101: 105030

Published Online 22

February 2024

[https://doi.org/10.](https://doi.org/10.1016/j.ebiom.2024.105030)

1016/j.ebiom.2024.

105030

Abbreviations: BOS, Bronchiolitis obliterans syndrome; CB, Constrictive bronchiolitis; CF, Cystic fibrosis; CLAD, Chronic lung allograft syndrome; DLCO, Diffusion capacity for carbon monoxide; FEV1, Forced expiratory volume in 1 s; FVC, Forced vital capacity; HRCT, High-resolution computed tomography; IPF, Idiopathic pulmonary fibrosis; OB, Obliterative bronchiolitis; RAS, Restrictive allograft syndrome; TLC, Total lung capacity

*Corresponding author. Department of Chronic Diseases, Metabolism and ageing (CHROMETA), Laboratory of Respiratory Diseases and Thoracic Surgery (BREATHE), KU Leuven and University Hospitals Leuven, Herestraat 49, B-3000, Leuven, Belgium.

E-mail address: robin.vos@uzleuven.be (R. Vos).

[†]Shared senior authorship.

Preliminary data from the present work was presented at the ISHLT Annual Meeting 2023, Denver, USA: Kerckhof P et al. *Morphometric Airway Changes in Explanted Human Lungs with Chronic Lung Allograft Dysfunction*, and the abstract was awarded with the ISHLT 2023 Research & Immunology Professional Community Award for Excellence.

Funding This research was funded with the National research fund Flanders (G060322N), received by R.V.

Copyright © 2024 The Authors. Published by Elsevier B.V. This is an open access article under the CC BY-NC-ND license (<http://creativecommons.org/licenses/by-nc-nd/4.0/>).

Keywords: Chronic lung allograft dysfunction (CLAD); Bronchiolitis obliterans syndrome (BOS); Restrictive allograft syndrome (RAS); Constrictive bronchiolitis; Airway tree; Obstruction

Research in context

Evidence before this study

Still much is unknown about how CLAD lungs are structurally affected. What we do know is that OB lesions are the main structural problem in BOS lungs, being located in the small airways. We furthermore have some idea about how spirometry reflects lung function in an abstracted way, i.e. FEV1 decline implies large-medium sized airway obstruction, FEF25-75 decline implies small airway obstruction. However, we still do not fully understand how airway lesions accumulate and add up together to result in the observed lung functions and eventually in death in patients with CLAD, as much of our knowledge is derived from isolated biopsies. One study therefore already investigated the airway tree as a whole, in end stage explanted BOS and RAS lungs. This way, the number of lesions in the proximal airways could be assessed. However, CT scans with a sub-optimal resolution (600 μm voxel size) were used, compared to what is now possible (155 μm voxel size). Furthermore, still no information about their impact on lung function was obtained.

Added value of this study

We performed an airway centred analysis of CLAD lungs, using whole lung μCT scans with a resulting voxel size of 155 μm , from which we could extract the airway tree to great detail. Airways were hereby charted up until a diameter of 0.6 mm, allowing detection of obstructions also in small airways and extrapolation of the functional backlash thereof. We thereby also included CLAD lungs of the mixed phenotype. We showed functional airways in BOS to be greatly declined, as opposed to previous research, in line with

spirometric lung function decline, while the mixed phenotype indeed demonstrated all BOS and RAS features.

We gave an overview of all lesions seen on μCT scans and compared these to their histological counterpart, to increase their μCT interpretability. Doing so, we also exposed mucus related airway lesions with different presentations, possibly being of more importance than commonly assumed. One similar lesion was once reported before as airway lesions with a thickness of only 48 μm . Lesions in BOS could furthermore be classified as mucus-related lesions and lesions which could best be described as constrictive bronchiolitis (CB), while these were continually present in airways ranging from 3.0 mm in diameter to the terminal bronchioles. Finally, the functional effect of airway lesions and their division throughout the lung was assessed. This revealed that end stage BOS lungs rely heavily on only one or a few distinct regions of the lung taking over most of the remaining functional ventilation.

Implications of all the available evidence

This research revealed that mixed CLAD lungs seem to be a combination of both BOS and RAS patterns, while both RAS and BOS also show features of one another, indicating CLAD to be a continuum of pathologies. The fact that BOS lungs appear to be affected regionally gives us insights on how BOS progresses and in what underlying mechanisms might be important therein. This can furthermore be related to lung function tests, to increase the interpretability of these in the specific CLAD setting. At last, our findings regarding mucus related lesions warrant increased attention to the role of mucus in the acute stages of CLAD.

Introduction

Chronic rejection after lung transplantation, also known as chronic lung allograft dysfunction (CLAD), affects up to 50% of patients within five years after transplantation and is the main cause of death after lung transplantation.¹ Most CLAD cases are caused by an obstructive pulmonary disease called bronchiolitis obliterans syndrome (BOS), while around 30% are affected by a restrictive pulmonary pattern, called restrictive allograft syndrome (RAS).² A minority of patients with CLAD develop a Mixed obstructive-restrictive defect, which is thus called a 'Mixed phenotype' and is most often preceded by a BOS phenotype.³ Rare CLAD cases inconsistent with these groups are currently

classified as 'undefined'.⁴ BOS is histologically characterized by air trapping due to scarring and intraluminal filling with fibro-collagenous tissue of the conducting bronchioles, often with sparing of large airways and alveolar surface.^{5,6} RAS is characterized by destruction of terminal bronchioles and alveolar interstitium with expansion of interstitial fibrous connective tissue, often with concomitant fibrosis of the adjacent visceral pleura.⁷ From current histologic studies in CLAD, it remains unclear how the changes in airway morphology and extent and nature of airway obstructions relate to regional ventilatory capacity within the lung. We therefore aimed to further characterize disease impact on airway lumina in both BOS, Mixed and RAS lungs, with

emphasis on the similarities and differences between phenotypes. For this, the entire airway tree of explanted human lungs was mapped using whole lung μ CT scanning, allowing digital 3D reconstruction and morphometric analysis of the airways to evaluate structural changes related to fibrotic remodelling in CLAD, and its effects on functional ventilatory capacity.

Methods

Lung processing and sampling

From our prospectively collected Biobank of human explant lungs, we identified 18 lungs (6 control, 6 BOS, 3 mixed and 3 RAS, according to the latest ISHLT consensus),⁸ which were matched for donor sex, age and height, and had sufficient quality for μ CT analysis (i.e. no gross infection, full insufflation at total lung capacity, TLC). Patient details were accessible through their online medical files. The mean explant date was 2/04/2017 with a standard deviation of 643 days. All lungs were cryopreserved as whole, inflated lungs at TLC, at -80°C as previously described.⁵ They subsequently underwent *ex vivo* whole lung μ CT scanning in these same conditions.⁵ μ CT setup (operated at voxel size $155\ \mu\text{m}$) was developed at Ghent University Centre for X-ray Tomography,⁹ as explained elsewhere.¹⁰ Control lungs consisted of unused donor lungs for transplantation, as previously described.^{3,5,7}

In addition, frozen tissue cores (2 cm height x 1.4 cm diameter) were obtained from these same lungs, and subsequently underwent μ CT scanning ($8.4\ \mu\text{m}$ voxel size, SkyScan 1172, SkyScan, Kontich, Belgium). A total of 30 tissue cores were scanned: nine cores from three control lungs, nine cores from three BOS lungs, six cores from two Mixed lungs and six cores from two RAS lungs. This allowed detailed visualization of small airway lesions, which is not possible with whole lung μ CT.

Airway data generation

ITK-Snap (version 3.8.0) was used for semi-automated 3D airway reconstruction from whole lung μ CT scans.¹¹ All airway lumina in contact with the main stem bronchus through open, non-occluded airways, were mapped up to a diameter of 0.6 mm (Fig. 1). Obstructed airways were identified by locating airways that did not continue to form daughter airways of the next generation. Airways downstream of a fully obstructed airway were not mapped and thus excluded for further research. In addition, all airways with a diameter of 0.6–1.2 mm (occurring after generation ten) were excluded (only) for analysis of obstructed airways, as their daughter airways could be too small to be detectable.

3D luminal airway casts were transformed to numerical data by NeuronStudio software (version 0.9.92),¹² which characterizes each airway segment

between two bifurcations (Fig. 1), by previously described methods.¹³ NeuronStudio provided length, average diameter and generation of each airway segment. These obtained results were represented in an orderly fashion, allowing to link each airway to its respective mother and daughter airway, to reconstruct the entire airway tree geometry.

Using this data, airway volume per generation can be calculated. To investigate airway volume increase per generation, the number of airways in the control lungs was matched to the number of airways per generation in the pathological lungs, where the smallest airways per generation of the control were not used as it was hypothesized and confirmed that these smallest airways in the pathological lungs are first to be obstructed. In this way, the same airways could be compared and bronchiectasis could be objectified.

Total airway volume, per lung, was calculated using R software on the segmented airways on the μ CT scans directly, based on voxel intensity of the coloured airways.

Statistics

R software (4.2.0) was used for all statistical analyses. The used statistical tests are indicated in the figure legends. Parametric tests (t-test, ANOVA, Dunnett) were used as the data comes from normally distributed populations. $p < 0.05$ was considered significant. Generally, mean \pm standard deviations are given, unless differently stated. Sample sizes were determined by availability and samples were matched, thus not using any randomization/blinding.

Ethics

This study was approved by the Ethics Committee UZ/KU Leuven (S51577, S52174, MP017200) and is in compliance with the ISHLT ethics statement. Informed consent was given for the use of patient tissue and data.

Role of funders

Funders had no active role in this research or the writing of this manuscript.

Results

Study cohort

Patient and lung characteristics per group are summarized in Table 1, with their infectious status in Table 2. The *in vivo* total lung volume evolution is found in Figure S1. An overview of the μ CT scans and airway tree of all included lungs can be found in Figure S2.

Of note, the Mixed CLAD lungs were obtained from patients initially diagnosed with a BOS phenotype, who had progressed to a Mixed phenotype. All CLAD lungs were obtained at end stage (CLAD stage four),⁴ during retransplantation or post-mortem autopsy, on average 6.7 years post-transplant. Last pulmonary function prior to lung explant procedure is summarized in Table 1.

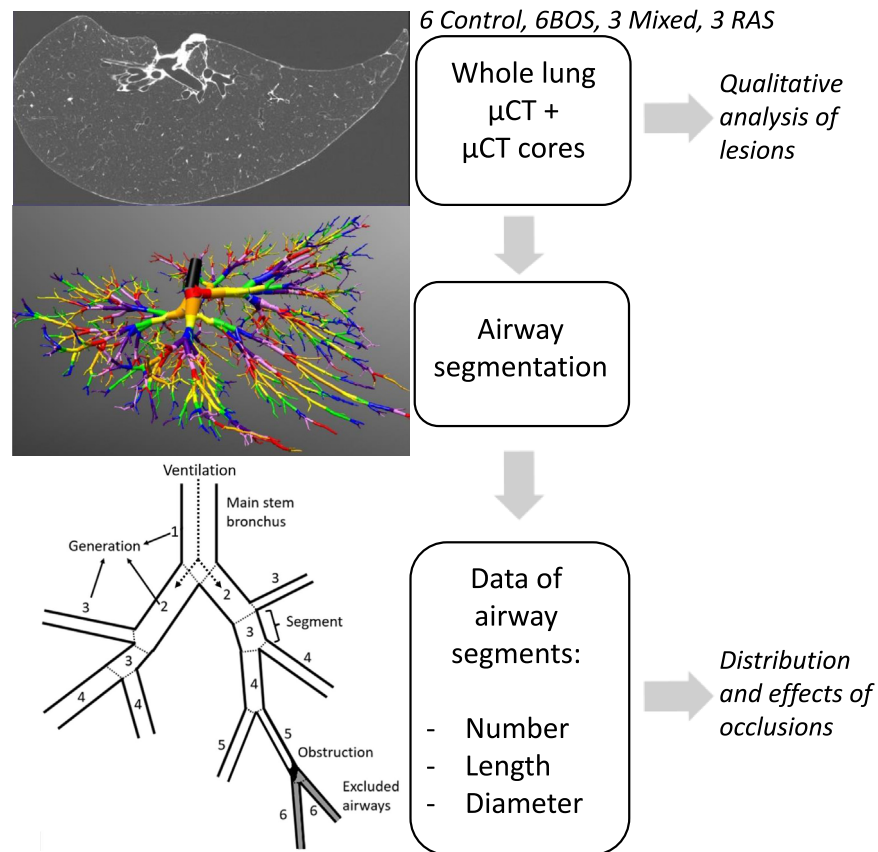


Fig. 1: General approach of the study. Whole lung μ CT scans were obtained, whilst additional μ CT cores were used to visualize bronchioles in 6 control, 6 BOS, 3 Mixed and 3 RAS lungs. Next, the airway tree was digitally reconstructed as a whole from the whole lung μ CT scans for quantitative analysis to evaluate the morphologic changes of the airway lumina. At the bottom left, an airway scheme is given with further details of the approach and used nomenclature.

Overall, whole lung μ CT showed mostly radiologically normal lung parenchyma in BOS, occasionally with interlobular septal thickening and discrete areas of peripleural attenuation, whereas in RAS various degrees of parenchymal and peri-pleural fibrosis were seen, with adjacent traction bronchiectasis of the larger airways (Fig. 2), consistent with literature.¹⁴

In vivo CT volumetry demonstrated a decreased lung volume in Mixed and RAS and an increased lung volume in BOS ($p = 0.07$, $p = 0.01$, $p = 0.11$, respectively, paired t-test). Mixed and RAS showed an increased lung density ($p < 0.0001$, Dunnet test), while only RAS showed an increased lung mass ($p = 0.0018$, Dunnet test) compared to controls (Table 1).

Patterns in airway lesions

Representative images of the airway tree in CLAD are shown in Fig. 2, demonstrating a less extensive airway tree (poor arborization) and distended airways (bronchiolectasis) mainly in BOS and the Mixed phenotype compared to controls.

From Fig. 3a, it is seen that the number of patent, not proximally obstructed, airways are significantly and similarly decreased in BOS and the Mixed phenotype and to a lesser extent in RAS. This is caused by the presence of airway obstructions, which are increasingly present with rising generations, starting from generation five (Fig. 3b) and causing about 50% of airways to be obstructed at generation 14 in BOS and the Mixed phenotype. This contrasts with RAS, where only about 20% of airways were obstructed at generation 14. There, obstructions arise mostly in the most distal mapped airways.

A typical view of the distal airways in BOS and RAS is shown in Fig. 3c and d, where a clear difference between BOS and RAS can be appreciated. BOS lungs had mostly normal respiratory bronchioles and often also normal terminal bronchioles, with, however, some specific obstructions (described further). In contrast, the small airways in RAS were often embedded in fibrosis, causing the airway lumen to become tortuous or even completely occluded. This occurred in respiratory

	Control	BOS	Mixed	RAS
Patients (n)	6	6	3	3
Sex m/f	3/3	3/3	1/2	2/1
Height (m)	1.70 (1.58–1.80)	1.67 (1.62–1.85)	1.68 (1.64–1.72)	1.69 (1.60–1.73)
Weight (kg)	75 (60–90)	46 (32–76)	54 (52–56)	58 (40–81)
Age recipient (years)	NA	45 (29–58)	55 (53–59)	53 (28–71)
Age donor (years)	57 (51–62)	40 (19–55)	49 (33–68)	50 (39–58)
Time to CLAD (years)	NA	3.6 (1.0–4.8)	2.9 (2.3–3.8)	4.5 (3.4–5.9)
Time to endpoint (years)	NA	6.8 (2.9–17.2)	7.2 (3.2–15.0)	6.1 (5.7–6.5)
Time to CLAD-endpoint	NA	3.2 (0.4–12.5)	4.4 (0.6–11.3)	1.6 (0.6–2.0)
Redo LTx/autopsy	NA	5/1	3/0	0/3
CF/PF/Emphysema/other (n)	NA	2/1/2/1	0/1/1/1	0/2/0/1
Last pulmonary function				
FEV1 (% pred)	NA	21 (12–32)	29 (23–38)	34 (24–53)
FEV1 (L)	NA	0.64 (0.30–1.05)	0.86 (0.79–0.93)	1.06 (0.75–1.62)
FVC (% pred)	NA	48 (34–64)	45 (27–61)	35 (25–55)
FVC (L)	NA	1.9 (1.1–3.3)	1.7 (1.2–2.6)	1.4 (0.9–2.2)
FEV1/FVC	NA	35 (27–51)	52 (31–67)	78 ^c (73–84)
TLC (% pred)	NA	91 (73–107)	70 (56–89)	66 (34–96)
DLCO (% pred)	NA	57 (38–76)	49 (40–56)	32 (19–50)
Left/right lung	3/3	2/4	2/1	3/0
Ex-vivo whole lung μCT				
Lung volume (L)	3.3 (2.5–4.2)	2.2 ^a (1.8–3.5)	1.2 ^c (0.8–1.6)	1.4 ^b (0.8–1.8)
Lung density (g/L)	89 (60–115)	138 (120–158)	327 ^c (228–480)	432 ^c (420–447)
Lung Mass (g)	291 (221–371)	297 (253–420)	369 (332–404)	607 ^b (344–767)
In vivo HRCT: Lung volume change (CLAD—pre-CLAD) (L)	NA	0.39 (–0.31 to 1.06)	–1.09 (–1.46 to –0.49)	–0.51 ^a (–0.61 to –0.40)

The data are represented as mean and range. Indications for transplantation were: Cystic fibrosis (CF), Pulmonary fibrosis (PF), Emphysema, histiocytosis X, Eisenmenger syndrome and RAS. The endpoint could be retransplantation or death of the patient. p-values are indicated as a difference with the control where possible and with BOS lungs if not, calculated with ANOVA with post-hoc Dunnet test. For the in vivo volume change, paired t-tests were performed comparing pre-CLAD volume with end-stage-CLAD volume, per group separately. ^ap < 0.05. ^bp < 0.01. ^cp < 0.001.

Table 1: Patient characteristics.

bronchioles and decreased in occurrence in more proximal airways.

The average number of non-obstructed airway segments with a diameter <1.2 mm was the lowest in

Mixed (149 ± 96) followed by BOS (220 ± 193) and RAS (729 ± 125), compared to controls (932 ± 382, p = 0.0041, 0.0017, 0.69 respectively, Dunnet test). This means that the number of residual functional small airway

	Azithromycin	Retransplant	Diagnostic tests	Infection
BOS1	Yes	Yes	Explant lung BAL: Candida Albicans	No
BOS2	Yes	Yes	Explant lung BAL: negative	No
BOS3	Yes	Yes	Explant lung BAL: negative	No
BOS4	No	Yes	Explant lung BAL: negative	No
BOS5	Yes	Yes	Explant lung BAL: negative	No
BOS6	Yes	Autopsy	Rx: negative	No
Mixed1	Yes	Yes	Explant lung BAL: negative	No
Mixed2	Yes	Yes	Explant lung BAL: negative	No
Mixed3	Yes	Yes	Explant lung BAL: negative	No
RAS1	No	Autopsy	Hemoculture: Pseudomonas, suggestive CT	Yes
RAS2	Yes	Autopsy	BAL: negative, suggestive Rx	Yes
RAS3	Yes	Autopsy	BAL: Aspergillus fumigatus complex, suggestive Rx	Yes

Azithromycin indicates administration in the pre-explant timeframe. Only the best available indicator for the presence of pathogens is given: broncho-alveolar lavage (BAL) is not always performed. With 'infection', lung infection is meant.

Table 2: Pathogen presence in the lungs at explant date.

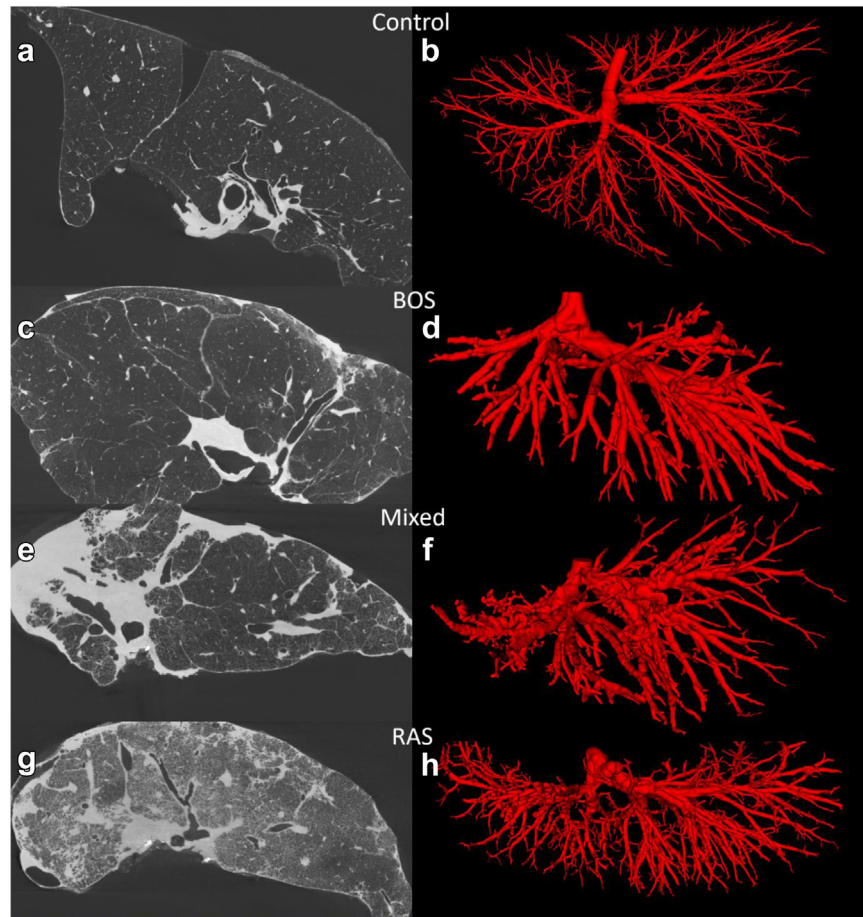


Fig. 2: Whole lung μ CT scans and reconstructed airways. (a, b) Lung parenchyma and total airway tree of a control (left lung), (c, d) BOS (right lung), (e, f) Mixed (Left lung) and (g, h) RAS (Left lung) lung.

segments (diameter <1.2 mm) was 16% in Mixed, 22% in BOS and 78% in RAS, respectively, compared to controls.

Taken together, BOS airways were increasingly obstructed with rising airway generation, while distal structures (alveoli, respiratory bronchioles, in part terminal bronchioles) remained mostly unaffected. RAS airways showed less obstructions in the proximal generations, while the most distal generations were severely affected. In Mixed phenotype, both patterns were observed, with some secondary pulmonary lobules (smallest functional unit of the lung) demonstrating similar observations as seen in BOS, while others matched with what was seen in RAS.

Typical airway lesions observed in BOS (also present in Mixed and less frequently in RAS) were further evaluated. First, airway diameter, rather than airway generation, appeared to be the main determinative factor for obstructions to occur (Fig. 4). It was typically the smallest of two sister airways which was preferentially obstructed ($p < 0.0001$, paired t-test) (Fig. 4a).

Arguments why this is an unbiased result are found in [Supplementary Material](#). Furthermore, in all CLAD subtypes, non-obstructed small airways were equally divided through the generations compared to the controls (Fig. 4b). This means that the generation itself does not determine the presence of obstructions. Airway obstructions are thus more likely to occur in airways with smaller diameters, and regardless of the generation to which they belong, all small airways are equally susceptible to these obstructions (“watershed” phenomenon).

This is explained in detail in [Figures S3](#) and [S4](#), also giving additional explanation of patterns in airway structure in CLAD and healthy lungs. As a result of obstructions occurring more frequently in the smallest airways, a ventilatory disequilibrium occurs within the lung: similar airway ‘branches’ (Fig. 5, [Figure S5](#) for more information) may aerate a variable number of distal respiratory bronchioles, depending on the number of proximally obstructed bronchioles (Fig. 5a–c, [Figure S4](#) for additional information). Mostly BOS, but

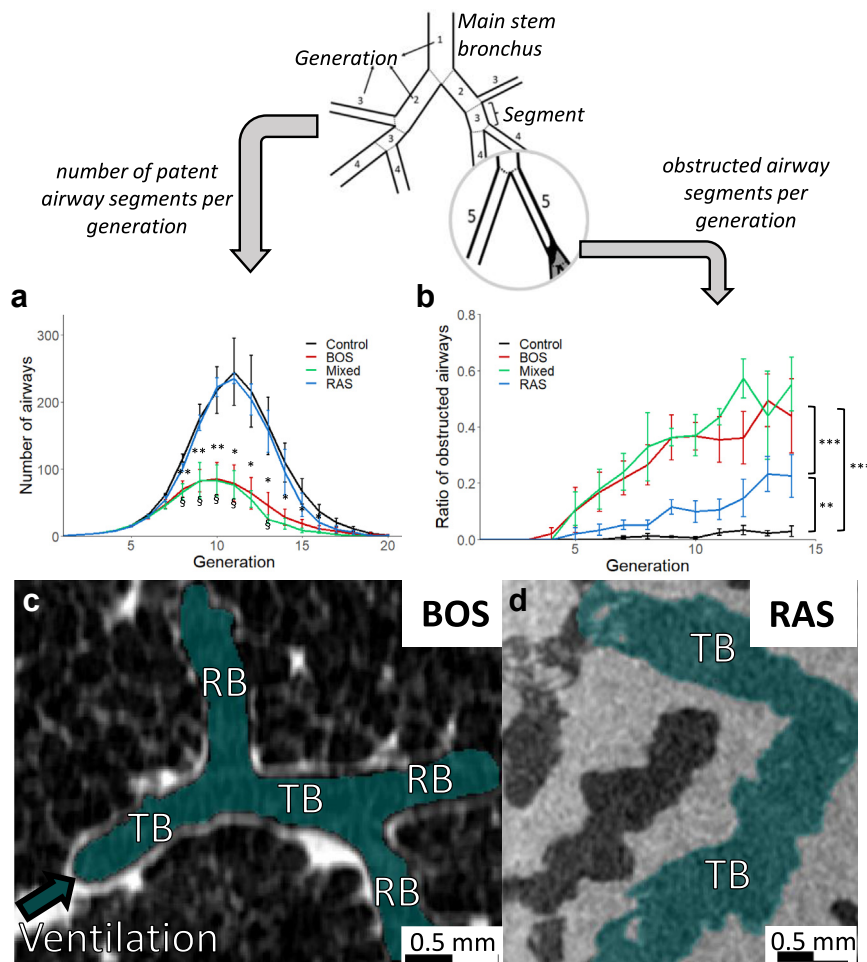


Fig. 3: Number of obstructions. (a) Number of non-occluded (open) airway segments per airway generation. Dunnett post-hoc test showed significant differences between BOS and control ($p < 0.05^*$, $p < 0.01^{**}$) and between Mixed and control ($p < 0.05^{\S}$) in some generations, as indicated in the figure. (b) Ratio (non-cumulative) of number of obstructed segments to the total number of segments per generation. Only the airway segments with a diameter >1.2 mm were used, to avoid bias by the resolution (See methods section). Multiple linear regression was performed to compare groups, including an interaction term between lung phenotype and generation, where generation was treated as a continuous variable. BOS and Mixed significantly differed from both RAS and controls ($p < 0.001^{***}$), while RAS also differed significantly compared to controls ($p < 0.01^{**}$). Error bars represent standard error of means. (c) Example of terminal bronchioles (TB) and respiratory bronchioles (RB) in BOS, showing a conserved anatomy. This is a typical representation, however TBs can be affected, while this is almost never the case for RBs. (d) Typical representation of RAS TBs caused by fibrosis, creating a tortuous airway. For Fig. 3a and b, sample sizes per generation are: Control: $n = 6$, BOS: $n = 6$, Mixed: $n = 3$, RAS: $n = 3$.

also Mixed phenotype, showed a significantly increased imbalance compared to controls, i.e. some branches aerate up to 33% of all remaining patent bronchioles, while other branches aerate 0%. This imbalance causes some parts of the lung to have absent or limited ventilation, which is similarly seen in RAS lungs, but to a lesser extent. There, the largest branches only account for the ventilation of 20% of the remaining bronchioles, total ventilation thus being more spatially balanced.

Additionally, airway branches that aerate the fewest number of bronchioles were the ones that contributed least to the functional ventilatory capacity, even before

onset of the disease. This is shown in Fig. 5d, where a positive correlation between *diameter* of a proximal airway branch and *number* of distal small bronchioles aerated by this branch is depicted for control and BOS lungs ($p = 10^{-12}$, $R^2 = 0.5$ and $p = 10^{-10}$, $R^2 = 0.4$, respectively, linear regression). Branches with a large diameter aerate a high percentage of distal bronchioles, as seen in control lungs. In BOS, it are the largest airway diameter branches which account for large parts of residual alveolar ventilation.

In addition to the observed spatial differences between branches, also the difference between upper and

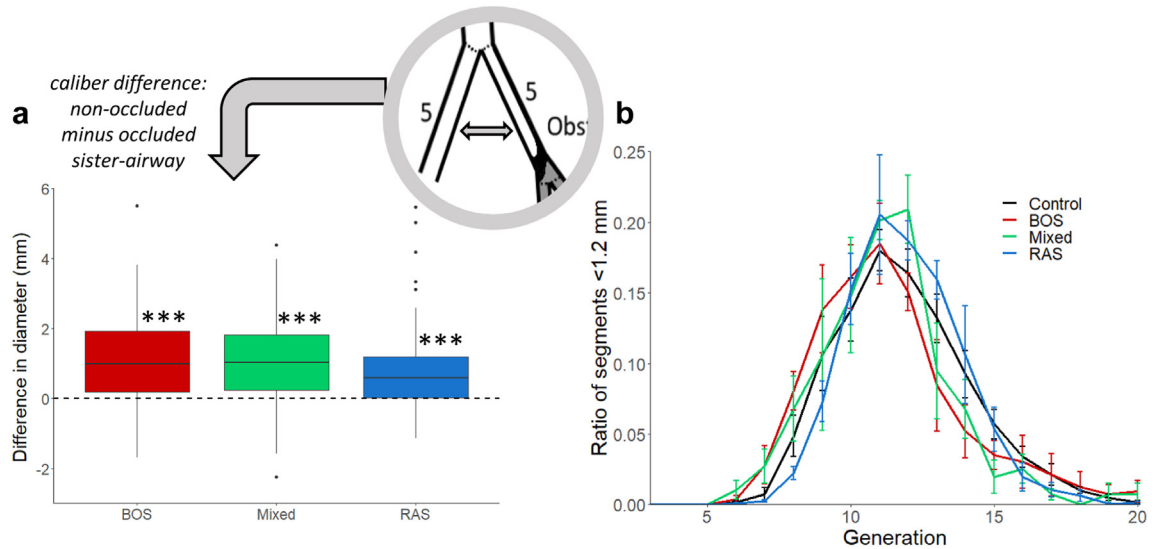


Fig. 4: Locality preference of obstructions (a) Comparison between the diameter of obstructed and non-obstructed daughter airway segments, showing that small (narrow) airways are preferably occluded. Only airways with a diameter >0.8 mm were used. A paired t-test was performed which showed significant differences from zero in all groups ($p < 0.001^{***}$). BOS: $n = 210$ pairs, Mixed, $n = 144$ pairs, RAS: $n = 108$ pairs. (b) Distribution of all remaining (functional) small bronchioles (diameter 0.8 – 1.2 mm). The y-axis shows the fraction of these bronchioles in a specific generation divided by the total number of these bronchioles in the lung, subsequently averaged per group. The similar distribution in all lungs shows that small airways are similarly affected, irrespective of what generation they belong to. Lung BOS-2 was excluded as there were almost no non-obstructed small airway segments left. ANOVA showed no significant differences for any given generation ($p > 0.05$) and that the occurrence of obstructions was not determined by the airway generation. Error bars represent standard error of means. Control: 6 lungs, 932 airway segments per lung, BOS: 6 lungs, 220 segments per lung, Mixed: 3 lungs, 149 segments per lung, RAS: 3 lungs, 729 segments per lung.

lower pulmonary lobes was assessed. The ratio between the number of non-obstructed bronchioles (diameter <1.2 mm) in the lower versus upper lobe was calculated. This ratio was 1.1 for controls, 3.1 for BOS, 1.2 for Mixed and 0.9 for RAS, indicating that obstructive lesions (in airways <1.2 mm in diameter) mainly affect the upper lobes in BOS compared to control lungs ($p = 0.069$, multiple linear regression corrected for L/R lung).

In non-obstructed airways, distended bronchioles (bronchiolectasis) were observed in all CLAD lungs, but mainly in BOS and Mixed phenotype. Total (luminal) airway volume, total airway volume per lung volume, and volume percentage of residual non-occluded airways in CLAD vs. control lungs are summarized in Fig. 6 and in the Supplementary Material. Even though lung volume was decreased in all CLAD lungs, total mapped (corrected) airway volume was increased.

On average, this increase in airway volume was approximately 50%. However, in Mixed and RAS lungs, this increase evolved into airway narrowing of the most distal airways (i.e., those beyond generation 12), indicating the presence of a constrictive process. This is further illustrated in Fig. 6c where the longest patent airway branch of 4 different lungs is shown, highlighting the airway dilatation in CLAD compared to controls.

Characterization of obstructive airway lesions

Obstructive airway lesions (obstructions) were present in bronchioles with a diameter of up to 3 mm, extending distally to the first generation respiratory bronchioles. In Fig. 7, CT images of different lesions are illustrated. Fig. 7b and c shows CT images of ‘bronchiolar webs’, which are thin structures often completely occluding the airway when assessed on CT. Fig. 7d shows an image likely to be a mucus plug. Fig. 7e shows a severely occluded lumen, which we would call an obliterative bronchiolitis (OB) lesion when only assessed on CT, while Fig. 7f and g shows CT images suggestive for constrictive bronchiolitis (CB). Fig. 8 shows a representative airway from a BOS core with multiple occlusions. Fig. 9b and c shows lymphocytic inflammation in the airway wall with marked neo-angiogenesis, extremely narrowing the airway lumen. Fig. 9d and e shows mucus stasis proximal to this lesion, containing mostly neutrophils and some eosinophils. Fig. 9g and h shows an airway which appears narrowed on CT with an obliterated branch, indicated by the continuous smooth muscle layer and absent lumen. This is an example of CB. On top of the airway we again see lymphocytic inflammation. Fig. 9j and k shows the histological correlate of a bronchiolar web: a fibrinous-mucinous structure containing a mixture of immune cells.

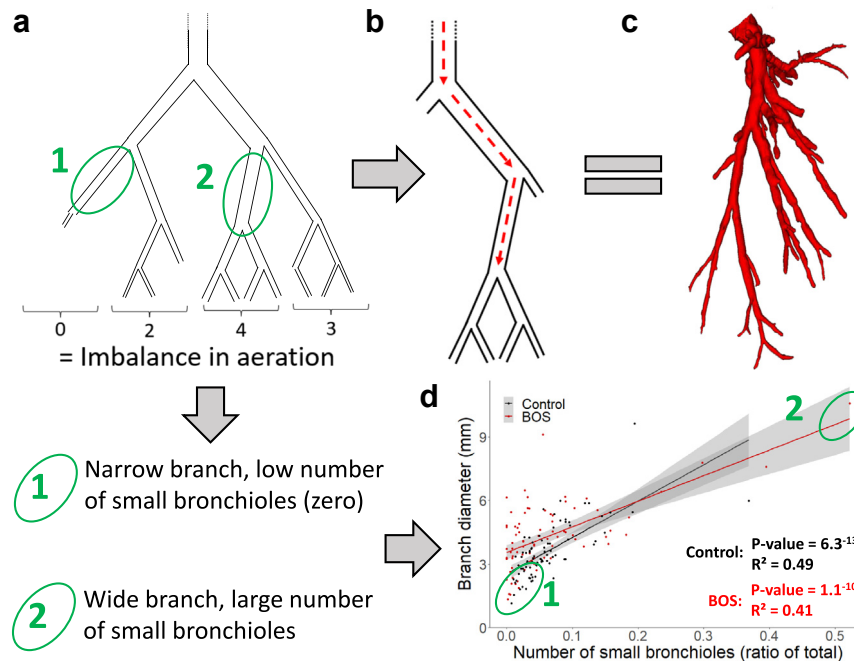


Fig. 5: Ventilation imbalance (a) Illustration of the origin of imbalance in lung ventilation in CLAD. Four equivalent airways ('branches') all aerate a different number of bronchioles. Further explanation is given in the online supplement (Figure S4). (b) The situation (imbalance) BOS and Mixed lungs evolve to, due to obstructions: one branch takes over most of the ventilation. (c) Real example of this phenomenon showing airways from a BOS lung. (d) Correlation between the width of the main airway of a branch and the number of small bronchioles that are present in this branch, distally. This is done for all BOS lungs and not RAS lungs, as we are here investigating effects of obstructions in airways >1.2 mm in diameter, typically found most in BOS lungs. Control: n = 96, BOS: n = 94, Pearson correlation shown.

Fig. 9m and n shows an axial view through an airway with CB, where the airway lumen is partly occluded by fibrosis. More distally, this airway was completely occluded (not shown). Additional CT and histological images are shown in Figures S6 and S7.

Most lesions were seen in BOS and Mixed phenotype, while the least lesions were observed in RAS. In RAS, lesions were more restricted to airways around the level of the terminal bronchioles and mostly absent in airways > 1 mm in diameter. Illustrative movies of these airway obstructions can be found in the online supplement.

Discussion

In the current study, the entire airway tree of explanted human lungs was mapped using whole lung μ CT scanning, which allowed 3D reconstruction and morphometric analysis of the airways, to evaluate structural changes related to remodelling in CLAD, and its effects on functional ventilatory capacity.

In particular, all CLAD phenotypes showed pathophysiological anomalies to some extent. Histological assessment showed the main type of obstructions in BOS to originate from inflammation in the airway wall resulting in CB. A clear predilection for the occurrence

of bronchiolar obstructions in the small diameter distal airways (proximal to the terminal bronchiole) was apparent, and proximal bronchi(ol)ectasis was present in all CLAD phenotypes. Most airway obstructions were seen in BOS compared to RAS, resulting in a significant reduction of residual functional airway segments and in ventilatory imbalance.

On ex-vivo whole lung μ CT images of CLAD lungs, airway lesions can be difficult to classify. Mucus plugs, airway wall inflammation and advanced airway fibrosis (CB or OB) cannot be easily discerned. On in vivo HRCT, lesions are even more difficult to assess and mostly only secondary effects like air trapping, airway wall thickening, and bronchiectasis can there be observed next to bronchiolar wall thickening.^{14,15} Thus, histological analysis remains the gold standard.

Histology showed all fibrotic lesions likely to originate from inside the airway wall. There is however ambiguity around the proper terms. The term OB and CB are historically used in different ways, and we will describe all these lesions as CB, consistent with, among others, Colby (1998) and retaining OB for a lumen-originating obliteration. These latter lesions were not found in our study, and neither in previous results from our lab, nor were these described by Colby (1998) to be associated with CLAD/BOS.^{5,16} Histology was able to

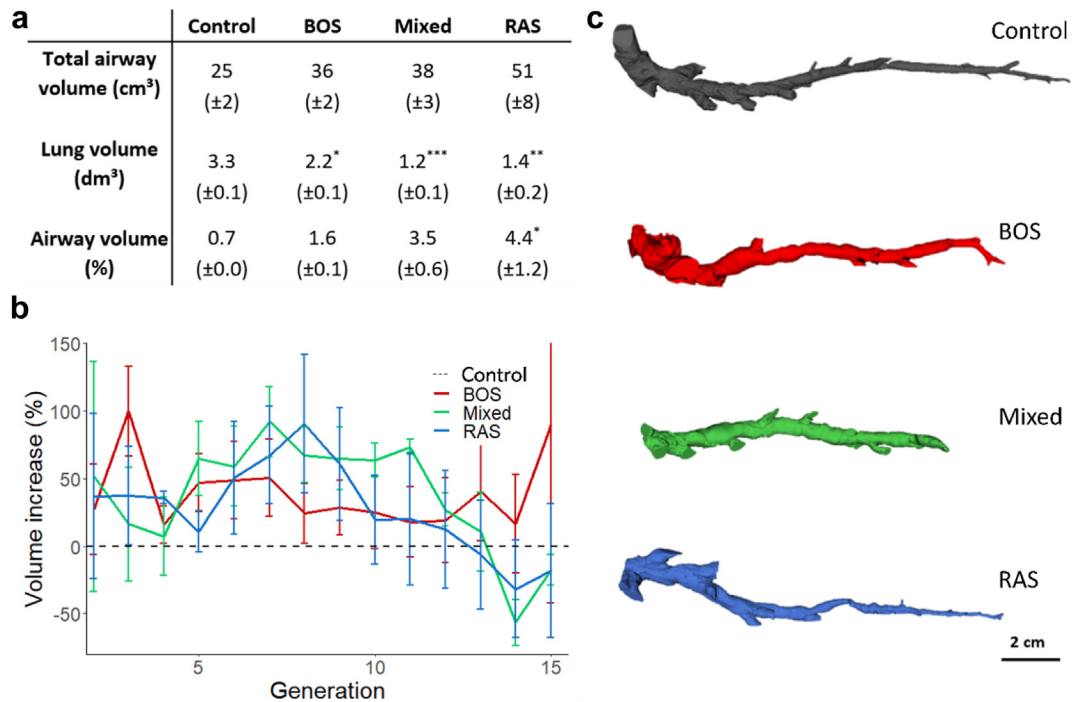


Fig. 6: Bronchi(ol)ectasis (a) The average of total airway volume, total lung volume and volume-percentage of (mapped) airways, standard deviation between brackets. ANOVA with Dunnett post-hoc test was performed ($p < 0.05^*$, $p < 0.01^{**}$, $p < 0.001^{***}$). (b) Average percentage of volume increase, or decrease, of all airway lumina per airway generation, for BOS ($n = 6$, per generation), Mixed ($n = 3$) and RAS ($n = 3$), relative to the control. Values above zero indicate bronchi(ol)ectasis. Error bars represent standard error of means. The airway volumes of the control lungs were corrected to match the loss of airways in BOS, Mixed and RAS, as explained in the supplementary methods. ANOVA for comparing each generation separately showed no significant differences ($p > 0.05$). (c) Illustration of the longest airway branch of 4 lungs. Bronchi(ol)ectasis can be seen in BOS and Mixed, while shortening of the branch is caused by occlusions and/or a decrease in lung volume.

discern lymphocytic inflammation, CB lesions and mucus plugs in BOS. Most likely, lymphocytic inflammation evolves over time, eventually leading to CB with a fully obstructed lumen, through fibrotic remodelling. The final endpoint is likely ‘vanishing airways’, where airways cannot be detected anymore.¹⁷ As described earlier, Lymphocytic airway inflammation was indeed previously proposed as a major driver of CLAD.¹⁸ Mucus plugs were often found, mostly in the vicinity of CB lesions, and were filled with neutrophils and some eosinophils, also being related to neutrophils in the airway wall. Interestingly, BOS is predominantly characterized by neutrophilic airway inflammation, mainly shown on BAL, possibly being related to infectious episodes.^{19,20} Possibly, these neutrophil-filled mucus plugs and concomitant infections predispose to airway remodelling, leading to CB lesions. Mucus was also present in thin structures obstructing the airway lumen, we defined as ‘bronchiolar webs’ on CT, which contained a mixture of immune cells, mainly neutrophils, imbedded in a fibrin matrix. It remains however largely unclear whether these webs play an important role in airflow obstruction and if these are transient or permanent in a CLAD setting. However, one previous example of webs

in a lung transplant setting was described in a case report of a two-year transplanted patient.²¹ There, these were called ‘bronchial webs’ as they were observed only in the bronchi, using bronchoscopy. It can however not be excluded that these bronchial webs were also present in the bronchioles. Similar to our results, these bronchial webs were comprised of a fibrin matrix filled with neutrophils. It remains thus unsure whether these webs have the same cause and whether they have the same airflow obstructing effect. One of our BOS lungs was seen to contain almost exclusively mucus plugs/webs causing airway obstruction, as assessed on μ CT. In this patient (BOS 2), there was a fast FEV1 decline (Figure S8), which required rapid retransplantation. We hypothesize that the observed bronchiolar lesions in this lung are therefore not yet fully consolidated (i.e. no organized fibrosis). This finding suggests that epithelial injury, airway inflammation and mucus formation could therefore play an important role in the initial stage of CLAD. All mentioned airway lesions are also present in RAS and Mixed lungs, as CT shows similar lesions in these lungs, be it to lesser extent.

We furthermore showed lesions to be present between airways with a diameter < 3 mm and more distally

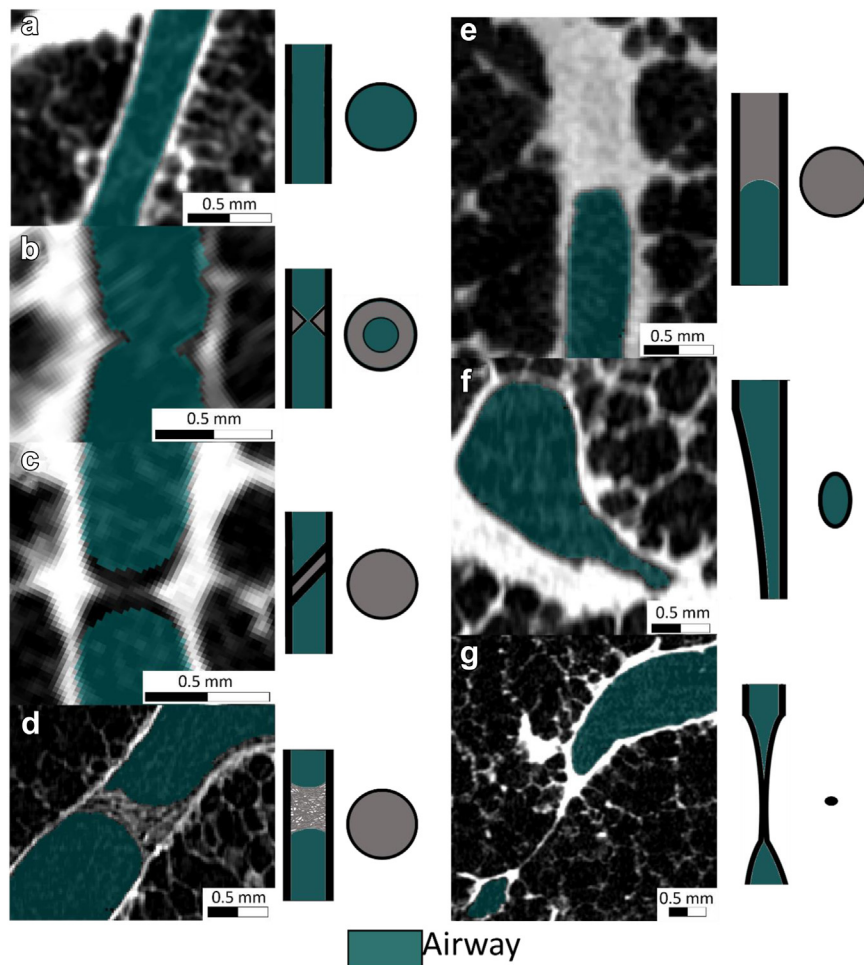


Fig. 7: Types of airway obstructions in BOS and RAS on μ CT cores, with corresponding illustrations in and perpendicular to the plane of the μ CT image. (a) Normal airway from a control lung. (b–c) Web: narrow incomplete to complete airway obstruction, when assessed on CT, caused by intraluminal mucus. (d) Mucus plug. (e) OB lesion as assessed on CT. Histologically, this could however be CB. (f–g) Constrictive bronchiolitis: airway narrowing.

the proximal respiratory bronchioles. In part, this coincides with previous findings stating the upper limit of diameter of affected airways to be 3.5 mm. It does however contradict previous findings stating that lesions are only present proximal to the terminal bronchioles, excluding the terminal bronchioles.⁵

Tortuous airways are a distinct cause of (partial or total) airway obstruction, only occurring in fibrotic regions (RAS and Mixed lungs), suggestive of traction bronchi(ol)ectasis. Previous research has demonstrated that in RAS, there is obstruction, constriction, and complete disappearance of bronchioles, which extends to the terminal bronchioles as indicated by μ CT analysis, consistent with our findings.⁷ Likely, alveolar/interstitial fibrosis in RAS^{2,22} results in constriction and even disappearance of these small airways.⁷

The number of open (non-obstructed) bronchioles was significantly lower in BOS compared to controls.

This difference was less pronounced in RAS, where the fibrotic process primarily affects the alveoli and inter-alveolar interstitium. In contrast, previous research by our group on lung tissue cores demonstrated that the number of open airways in BOS was comparable to controls, while this was severely decreased in RAS.⁷ This difference may be due to a different approach in calculating the number of functioning airways. In the present study, non-obstructed (open) airways were visualized using whole lung μ CT and airways distal to (complete) obstructions were excluded for analysis (while airways with partial luminal obstruction were retained). Additionally, sampling of the tissue cores could influence these results. Previously, we used μ CT imaging and histology of lung cores to assess the number of open airways, also including visible airways (including CB airway remnants) distal to obstructions.⁷ The latter, however, does not take into account that seemingly

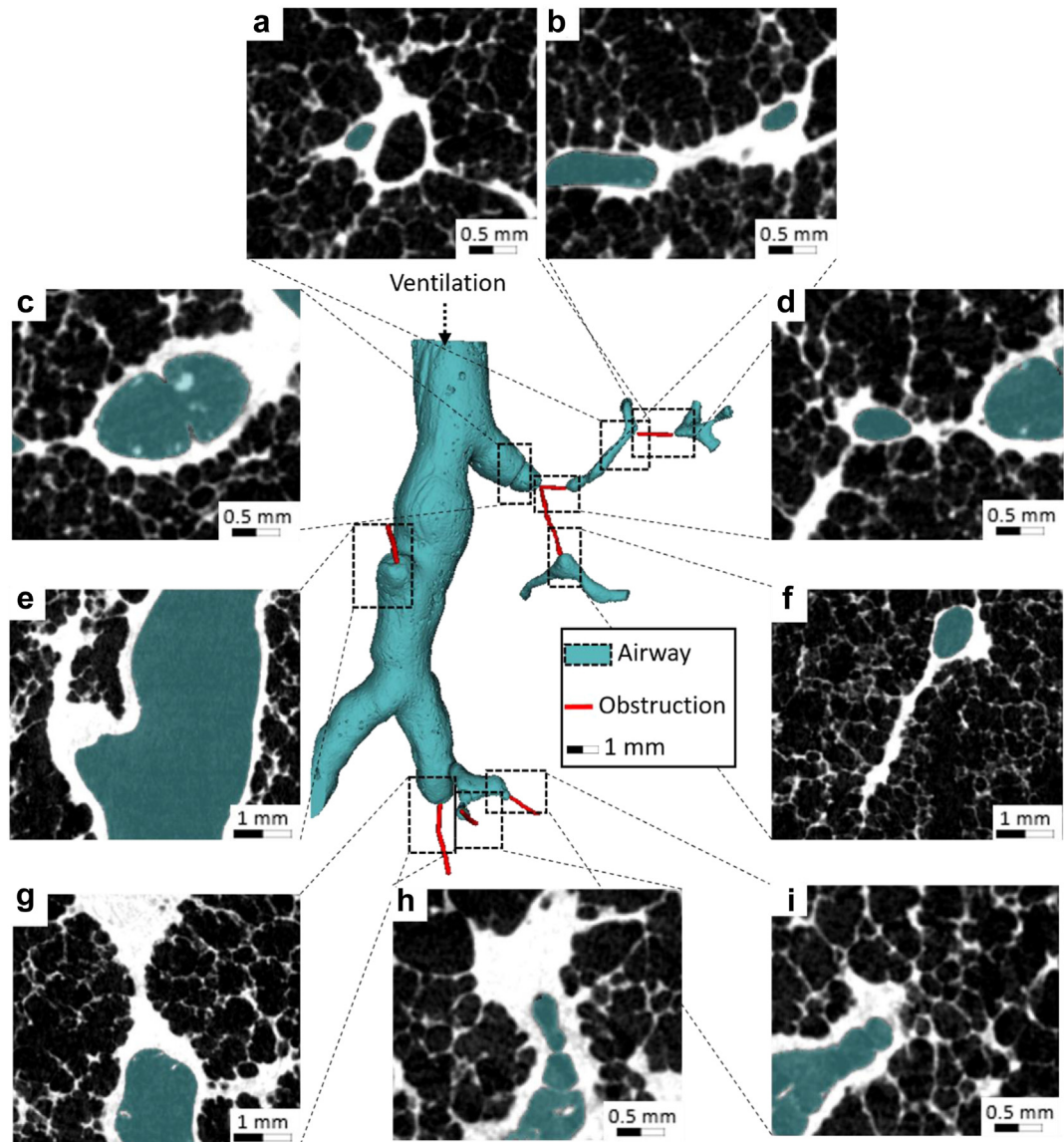


Fig. 8: Airway tree from a BOS core with CT images of all observed lesions. (a) Narrowed airway (CB). (b) Example of CB. (c) Example of a web. (d) Example of CB. (e) Example of CB in a relatively large airway. (f–i) examples of CB with some webs in h–i.

unaffected airways could be affected more proximally, leading to a partial or complete loss of function. These two methods are illustrated in [Figure S9](#).

Interestingly, lungs with Mixed phenotype demonstrated airway obstructions resembling those seen in BOS (both in number and nature), while RAS lungs only had substantial airway obstructions in the most distal airways (generation >12). These findings appear to relate to the clinical evolution of these patients over time, as Mixed phenotype patients had evolved from a BOS phenotype to a RAS phenotype over time, while none of the patients with RAS previously had clinical BOS preceding their RAS diagnosis. The large decrease

in number of functional airways in RAS in our prior research again contrasts our current findings in RAS, but not those in the Mixed phenotype.⁷ Besides differences in analysis, as described before (lung tissue cores vs. whole lung μ CT), another possible explanation could thus be that RAS lungs from prior research also showed BOS features (i.e. clinical BOS to RAS evolution). Indeed 4/9 of those RAS lungs could retrospectively be defined as a Mixed phenotype.

The most frequently obstructed airways in all CLAD phenotypes are those with the smallest diameter, extending distally to the terminal bronchioles. This preference was independent of airway generation. Since

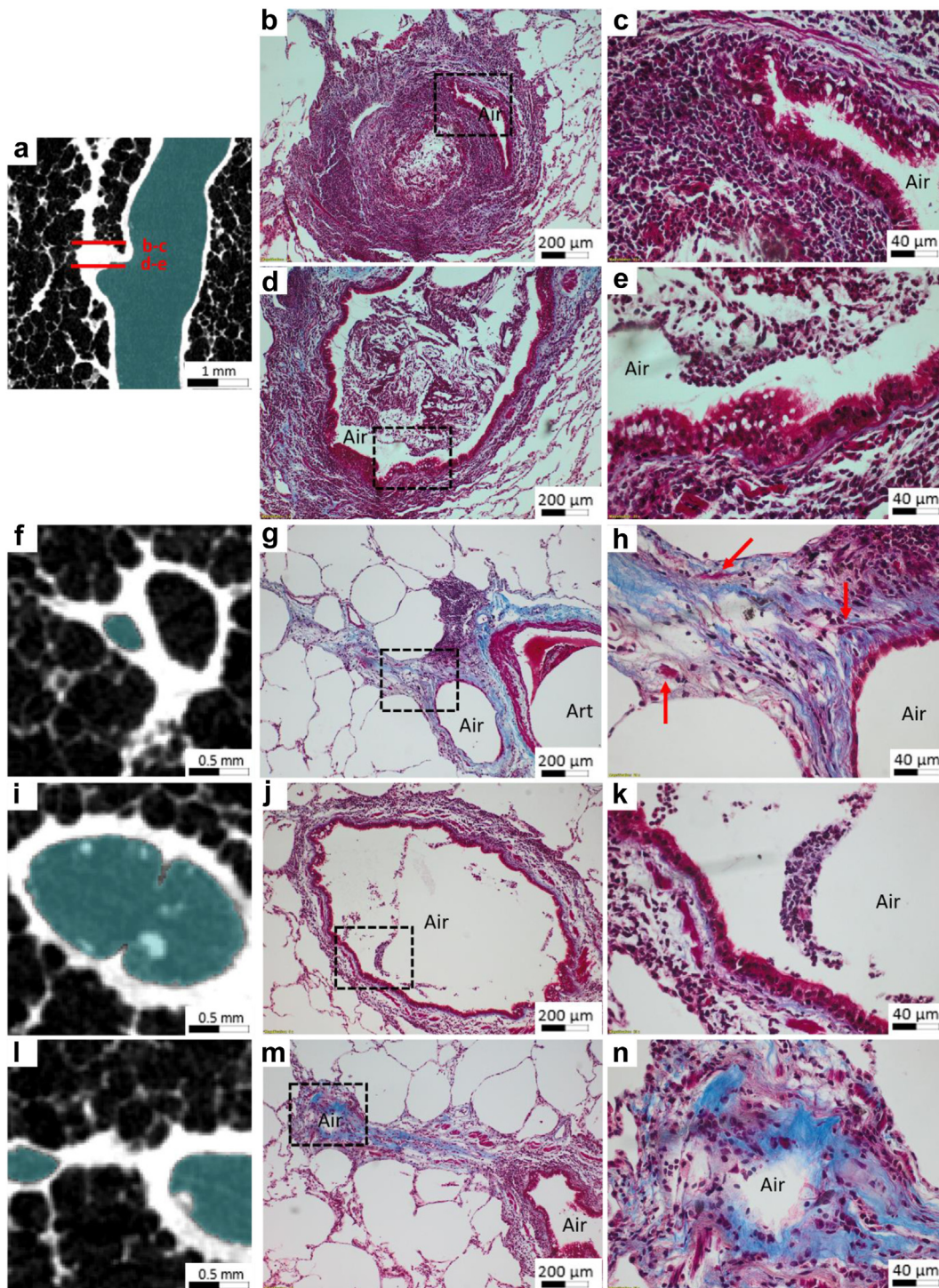


Fig. 9: Masson's trichrome staining on some of the lesions of Fig. 8. (a–e) Lymphocytic inflammation with neo-angiogenesis and an extremely narrowed airway lumen. Proximally, we see luminal mucus stasis filled with neutrophils and some eosinophils. (f–h) Constrictive bronchiolitis of a side branch seen in Fig. 9f where the lumen has disappeared. Red arrows show smooth muscle, indicating that this is an occluded bronchiole. Lymphocytic inflammation is seen on top of the airway in Fig. 9g. (i–k) Example of a web: fibrinous-mucinous matrix filled with various immune cells. (l–n) Constrictive bronchiolitis with collagen deposition and lack of airway epithelium. Air, airway; Art, artery. Red lines show where slices are taken.

airway *diameter*—rather than airway *generation*—relates to the relative distance from the terminal bronchioles, spatial proximity between a specific point within the airway and the more distal terminal bronchioles thus appears to be the determinative factor for the occurrence of airway obstructions.²³

It was hypothesized in previous research that obstructive lesions in CLAD result from microvascular damage and ischemia, which may be associated with permanent disruption of bronchial artery blood supply, as there is no anastomosis of the bronchial circulation, after lung transplantation (“watershed” phenomenon).²⁴ Bronchial arteries provide nutrients and oxygen to the conducting airways, as far as the terminal bronchioles, while more distal structures only rely on pulmonary arterioles, originating from the pulmonary artery.²⁵ Disruption of the bronchial circulation thus results in hypoxemia of a watershed area (including the terminal bronchioles situated proximal to the respiratory bronchioles), whereas the more distal structures (respiratory bronchioles and alveoli) remain perfused. These distal structures appear to be largely unaffected by airway obstructions in our BOS lungs (~bronchial circulation), while it are these regions which are primarily affected in RAS lungs (~systemic circulation). Clinically, bronchial artery revascularization at the time of lung transplantation has demonstrated to result in less BOS in children,²⁶ or to postpone the onset of BOS in adults,^{27,28} supporting this hypothesis. Later, additional injuries to the bronchiolar epithelium, caused by various harmful events such as infection or rejection post-transplant, may result in new obstructive airway lesions, which thus explains the different pathological stages—and heterogeneity—of the observed airway lesions in our study.

Likely, all observed airway lesions cause a pressure increase in the airways, which could be the cause of bronchi (ol)ectasis, as indeed many non-occluded bronchioles were shown to be dilated in CLAD, confirming previous research which demonstrated that the diameter of medium sized airways (generation seven to ten) was increased in BOS.²⁹

The presence of non-uniformly distributed airway obstructions in CLAD creates a ventilatory imbalance, leading to inadequate ventilation in certain areas of the lung. This can result in obstructive atelectasis and pulmonary shunting downstream of the affected secondary pulmonary lobules, which clinically relates to reduced airflow, desaturation, and can also affect the distribution of inhaled particles (such as those administered through nebulization) in established CLAD. However, retro-obstructive air-filled bronchioles were currently and previously visualized, which may be due to collateral ventilation through remaining interalveolar pores of Kohn, bronchiole-alveolar (Lambert’s channels) and inter-bronchiolar (Martin’s channels) communications, a physiologic mechanism to prevent alveolar atelectasis downstream from an obstruction. Interestingly, we

previously demonstrated an approximately threefold increase in interalveolar pore numbers in BOS compared to aging non-BOS controls,³⁰ which may be the result of compensatory dilatation of these pores secondary to the increased pressure in unaffected airways.

In conclusion, our results suggest that different pathophysiological conditions/disease processes seen in the distinct clinical CLAD phenotypes (i.e. BOS, Mixed, RAS) are present within all CLAD lungs, but to a variable extent. Constrictive bronchiolitis with fibrotic remodelling seems to be the major histological correlate of bronchiolar obstructions in BOS and likely partly in Mixed and RAS lungs. The observed changes in airway morphology explain how pulmonary function is affected in CLAD. It is important for future research to further characterize the molecular nature of the observed CLAD lesions, in which spatial transcriptome analysis of regions of interest could play an important role.

Limitations

These results are based on a static, inflated lung. A dynamic in- and expiratory setup could give additional ventilatory insights. Furthermore, whole lung μ CT and core μ CT are de-coupled, preventing accurate representation of alveolar ventilation as large airways cannot be followed to the alveolar level. Lastly, the number of included lungs is limited.

Contributors

Pieterjan Kerckhof: Resources, conceptualization, data curation, investigation, formal analysis, writing original draft, visualisation.

Gene PL. Ambrocio: Data curation.

Hanne Beeckmans: Resources, review & editing.

Janne Kaes: Resources, review & editing.

Vincent Geudens: Resources, review & editing.

Saskia Bos: Resources, review & editing.

Lynn Willems: Resources, review & editing.

Astrid Vermaut: Resources.

Marie Vermant: Resources, review & editing.

Tinne Goos: Resources, review & editing.

Charlotte De Fays: Resources.

Lucia Aversa: Resources.

Yousry Mohamady: Resources.

Arno Vanstapel: Resources, review & editing, validation.

Michaela Orlitová: Resources, review & editing.

Jan Van Slambrouck: Resources, review & editing.

Xin Jin: Resources.

Vimi Varghese: Resources, review & editing.

Iván Josipovic: Resources.

Matthieu N. Boone: Resources, review & editing.

Lieven J. Dupont: Resources.

Birgit Weynand: Resources, validation.

Adriana Dubbeldam: Resources, validation.

Dirk Van Raemdonck: Resources, review & editing.

Laurens J. Ceulemans: Resources.

Ghislaine Gayan-Ramirez: Resources, review & editing.

Laurens J. De Sadeleer: Resources, review & editing.

John E. McDonough: Resources, review & editing.

Bart M. Vanaudenaerde: Conceptualization, supervision, review & editing, validation.

Robin Vos: Conceptualization, supervision, funding acquisition, review & editing, validation.

All authors read and approved the final version of the manuscript.

Data sharing statement

Numerical data from airway segmentation (Neuronstudio output), is available upon request.

Declaration of interests

JK and VG and MV are junior research fellows of the Research Foundation Flanders (FWO; 1198920N and 1102020N and 1SE433N). MV received compensation from Sanofi for attending the ERS 2023 congress. GPLA is supported by an European Respiratory Society Clinical Fellowship Grant. SB is supported by the Paul Corris International Clinical Research Training Scholarship. LJDS (De Sadeleer) is supported by the European Union's Horizon Europe research and innovation programme as a Marie Skłodowska-Curie actions post-doctoral fellowship (grant agreement No. 101066289).

Acknowledgements

This research was funded with the National research fund Flanders (G060322N), received by R.V.

- RV is a Senior Clinical Research Fellow of the Research Foundation Flanders (FWO; 12G8715N) and supported by a research grant from FWO (G060322N).

- BMV is supported by a KU Leuven grant (C16/19/005).

- IJ is supported by the Ghent University Special Research Fund (BOF.EXP.2017.0007 and BOF.COR.2022.0009).

Appendix A. Supplementary data

Supplementary data related to this article can be found at <https://doi.org/10.1016/j.ebiom.2024.105030>.

References

- Bos S, Vos R, Van Raemdonck DE, Verleden GM. Survival in adult lung transplantation: where are we in 2020? *Curr Opin Organ Transplant*. 2020;25(3):268–273. <https://doi.org/10.1097/MOT.0000000000000753>.
- Verleden SE, Vos R, Vanaudenaerde BM, Verleden GM. Chronic lung allograft dysfunction phenotypes and treatment. *J Thorac Dis*. 2017;9(8):2650–2659. <https://doi.org/10.21037/jtd.2017.07.81>.
- Verleden SE, Von Der Thüsen J, Van Herck A, et al. Identification and characterization of chronic lung allograft dysfunction patients with mixed phenotype: a single-center study. *Clin Transplant*. 2020;34(2). <https://doi.org/10.1111/ctr.13781>.
- Verleden GM, Glanville AR, Lease ED, et al. Chronic lung allograft dysfunction: definition, diagnostic criteria, and approaches to treatment—A consensus report from the Pulmonary Council of the ISHLT. *J Heart Lung Transplant*. 2019;38(5):493–503. <https://doi.org/10.1016/j.HEALUN.2019.03.009>.
- Verleden SE, Vasilescu DM, Willems S, et al. The site and nature of airway obstruction after lung transplantation. *Am J Respir Crit Care Med*. 2014;189(3):292–300. <https://doi.org/10.1164/rccm.201310-1894OC>.
- Parulekar AD, Kao CC. Detection, classification, and management of rejection after lung transplantation. *J Thorac Dis*. 2019;11(Suppl 14):S1732–S1739. <https://doi.org/10.21037/jtd.2019.03.83>.
- Verleden SE, Vasilescu DM, McDonough JE, et al. Linking clinical phenotypes of chronic lung allograft dysfunction to changes in lung structure. *Eur Respir J*. 2015;46(5):1430–1439. <https://doi.org/10.1183/09031936.00010615>.
- Glanville AR, Verleden GM, Todd JL, et al. Chronic lung allograft dysfunction: definition and update of restrictive allograft syndrome—A consensus report from the Pulmonary Council of the ISHLT. *J Heart Lung Transplant*. 2019;38(5):483–492. <https://doi.org/10.1016/j.healun.2019.03.008>.
- Srivastava AK, Sharma M, Lau BK, et al. HECTOR: a 240kV micro-CT setup optimized for research. *J Phys Conf Ser*. 2013;463(1):012012. <https://doi.org/10.1088/1742-6596/463/1/012012>.
- Everaerts S, McDonough JE, Verleden SE, et al. Airway morphometry in COPD with bronchiectasis: a view on all airway generations. *Eur Respir J*. 2019;54(5). <https://doi.org/10.1183/13993003.02166-2018>.
- Yushkevich PA, Piven J, Hazlett HC, et al. User-guided 3D active contour segmentation of anatomical structures: significantly improved efficiency and reliability. *Neuroimage*. 2006;31(3):1116–1128. <https://doi.org/10.1016/j.neuroimage.2006.01.015>.
- Wearne SL, Rodriguez A, Ehlenberger DB, Rocher AB, Henderson SC, Hof PR. New techniques for imaging, digitization and analysis of three-dimensional neural morphology on multiple scales. *Neuroscience*. 2005;136(3):661–680. <https://doi.org/10.1016/J.NEUROSCIENCE.2005.05.053>.
- Rodriguez A, Ehlenberger DB, Dickstein DL, Hof PR, Wearne SL. Automated three-dimensional detection and shape classification of dendritic spines from fluorescence microscopy images. *PLoS One*. 2008;3(4):1997. <https://doi.org/10.1371/JOURNAL.PONE.0001997>.
- Byrne D, Nador RG, English JC, et al. Chronic lung allograft dysfunction: review of CT and pathologic findings. *Radiol Cardiothorac Imaging*. 2021;3(1). <https://doi.org/10.1148/RYCT.2021.200314>.
- Hota P, Dass C, Kumaran M, Simpson S. High-resolution ct findings of obstructive and restrictive phenotypes of chronic lung allograft dysfunction: more than just bronchiolitis obliterans syndrome. *Am J Roentgenol*. 2018;211(1):W13–W21. <https://doi.org/10.2214/AJR.17.19041>.
- Colby TV. Bronchiolitis: pathologic considerations. *Am J Clin Pathol*. 1998;109(1):101–109. <https://doi.org/10.1093/AJCP/109.1.101>.
- Vanstapel A, Verleden SE, Verbeken EK, et al. Beyond bronchiolitis obliterans: in-depth histopathologic characterization of bronchiolitis obliterans syndrome after lung transplantation. *J Clin Med*. 2021;11(1). <https://doi.org/10.3390/JCM11010111>.
- Santos J, Calabrese DR, Greenland JR. Lymphocytic airway inflammation in lung allografts. *Front Immunol*. 2022;13. <https://doi.org/10.3389/FIMMU.2022.908693>.
- Verleden GM, Vos R, De Vleeschauwer SI, et al. Obliterative bronchiolitis following lung transplantation: from old to new concepts? *Transpl Int*. 2009;22(8):771–779. <https://doi.org/10.1111/j.1432-2277.2009.00872.X>.
- Mamessier E, Milhe F, Badier M, Thomas P, Magnan A, Reynaud-Gaubert M. Comparison of induced sputum and bronchoalveolar lavage in lung transplant recipients. *J Heart Lung Transplant*. 2006;25(5):523–532. <https://doi.org/10.1016/j.healun.2005.12.009>.
- Keating DT, Westall GP, Pham A, Whitford HM, Williams TJ, Snell GI. Proliferating bronchial webs after lung transplantation. *Ann Thorac Surg*. 2011;92(5):1893–1896. <https://doi.org/10.1016/j.ATHORACSUR.2011.05.033>.
- Gauthier JM, Hachem RR, Kreisel D. Update on chronic lung allograft dysfunction. *Curr Transplant Rep*. 2016;3(3):185–191. <https://doi.org/10.1007/S40472-016-0112-Y>.
- Horsfield K. Diameters, generations, and orders of branches in the bronchial tree. *J Appl Physiol*. 1990;68(2):457–461. <https://doi.org/10.1152/JAPPL.1990.68.2.457>.
- Gauthier JM, Ruiz-Pérez D, Li W, et al. Diagnosis, pathophysiology and experimental models of chronic lung allograft rejection. *Transplantation*. 2018;102(9):1459. <https://doi.org/10.1097/TP.0000000000002250>.
- Baile EM. The anatomy and physiology of the bronchial circulation. *J Aerosol Med*. 1996;9(1):1–6. <https://doi.org/10.1089/jam.1996.9.1>.
- Guzman-Prunedo FA, Orr Y, Trost JG, et al. Bronchial artery revascularization and en bloc lung transplant in children. *J Heart Lung Transplant*. 2016;35(1):122–129. <https://doi.org/10.1016/j.HEALUN.2015.08.010>.
- Nørgaard MA, Andersen CB, Pettersson G. Does bronchial artery revascularization influence results concerning bronchiolitis obliterans syndrome and/or obliterative bronchiolitis after lung transplantation? *Eur J Cardio Thorac Surg*. 1998;14(3):311–318. [https://doi.org/10.1016/S1010-7940\(98\)00182-1](https://doi.org/10.1016/S1010-7940(98)00182-1).
- Pettersson GB, Karam K, Thuita L, et al. Comparative study of bronchial artery revascularization in lung transplantation. *J Thorac Cardiovasc Surg*. 2013;146(4). <https://doi.org/10.1016/j.JTCVS.2013.04.030>.
- Vanstapel A, Weynand B, De Zutter A, et al. Phenotypical characterization of airway morphology in post-infectious vs post-lung transplantation bronchiolitis obliterans. *J Heart Lung Transplant*. 2021;40(4):S36. <https://doi.org/10.1016/j.HEALUN.2021.01.1826>.
- Vanstapel A, Weynand B, Kaes J, et al. Interleaved pores increase in aging and severe airway obstruction. *Am J Respir Crit Care Med*. 2021;204(7):862–865. <https://doi.org/10.1164/RCCM.202102-0530LE>.